Proceedings of the Sixteenth International Conference on
Computational Structures Technology
Edited by: P. Iványi, J. Kruis and B.H.V. Topping
Civil-Comp Conferences, Volume 14, Paper 12.1
Civil-Comp Press, Edinburgh, United Kingdom, 2026
ISSN: 2753-3239, doi: 10.4203/ccc.14.12.1

Simultaneous Optimization of Ply Angles and Thickness for Double-Double Laminates

P. Fang, T. Gao and W. Zhang

State IJR Center of Aerospace Design and Additive Manufacturing, Northwestern Polytechnical University, Xi'an, China

Abstract

Double-Double (DD) laminates facilitate high-performance and lightweight designs through ply angle optimisation and gradual thickness tapering. This work proposes a simultaneous optimisation method for ply angles and thickness of Double-Double (DD) laminates. The Progressive Ply Interpolation[1] (PPI) model is improved through two key modifications. First, the weight expression is streamlined by simplifying the product terms of design variables from underlying sub-plies. This modification reduces the computational cost for both interpolation and sensitivity analysis. Second, angle optimisation is integrated into the interpolation scheme to facilitate simultaneous design of angles and thickness. Additionally, two penalty strategies are developed to enforce discrete ply angles. Numerical results confirm the ability to obtain discrete angles, thereby achieving the concurrent optimisation design of discrete angles and thickness for DD laminates.

Keywords: Composite materials; Double-Double laminates; Progressive Ply Interpolation model; Ply-drop; Angle and thickness optimisation design; Stiffness optimisation design

1 Introduction

Tsai [2]introduced the Double-Double (DD) laminate concept as an innovative alternative to conventional stacking sequences. Characterized by repeated sub-plies containing two pairs of balanced angles [±Φ/±Ψ], this architecture yields superior bending homogeneity compared to standard Quad laminates restricted to 0°, ±45°, and

90° orientations. Such configurations satisfy critical design constraints while retaining the simplicity of a four-ply sub-ply unit. Furthermore, the inherent modularity of DD laminates facilitates lightweight structures with gradual thickness tapering. This capability stems from the card sliding mechanism illustrated in Fig. 1, which allows for efficient thickness adjustments [3,4]. These advantages have attracted significant attention from both academic and industrial communities, highlighting the potential for broader application in composite structures.

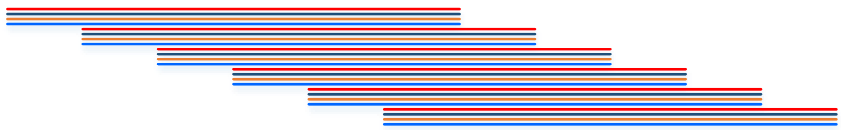

Figure 1: The "card sliding" technique of DD laminates.

To maintain structural homogeneity, thickness variations in DD laminates are typically defined in units of single sub-plies. Existing literature primarily addresses thickness optimisation. Tsai [3] developed the LAMSEARCH method specifically for DD laminate thickness design. Shrivastava et al.[5] utilized genetic algorithms to replace traditional Quad laminates with DD configurations, optimizing wing mass under failure and buckling criteria. David et al.[6] established a formulation and optimisation strategy for DD composites, demonstrating computational efficiency and manufacturing compliance in wing box applications. Wang et al. [7] introduced an implicit model to optimize thickness tapering, focusing on buckling resistance within weight limits. To the authors' knowledge, gradient-based methods for simultaneous optimisation of ply angles and thickness of DD laminates are still rare at this stage; therefore, a method enabling concurrent optimisation of thickness and angles for DD laminates is urgently needed.

2 Methods

This section presents the improved Progressive Ply Interpolation (PPI) model, the relationship between continuous ply angles and laminate stiffness, and the formulation of the discrete angle penalty strategy.

2.1 Improved Progressive Ply Interpolation (PPI) model

To satisfy the requirements for discrete sub-ply numbers, absence of empty sub-plies, and gradual thickness tapering in variable thickness DD laminate design, this work employs the differences in laminate stiffness matrices as the interpolation object.

The difference in the laminate stiffness matrix is expressed as the difference between the laminate *j*th and the laminate *j*-1th. We perform interpolation on this difference in the laminate stiffness matrix. The differences of the laminate **A B D** matrix of sub-ply *j*th can be expressed as:

$$\begin{bmatrix} \Delta\mathbf{A} & \Delta\mathbf{B} \\ \Delta\mathbf{B} & \Delta\mathbf{D} \end{bmatrix}^{(j)} = \begin{bmatrix} \mathbf{A} & \mathbf{B} \\ \mathbf{B} & \mathbf{D} \end{bmatrix}^{(j)} - \begin{bmatrix} \mathbf{A} & \mathbf{B} \\ \mathbf{B} & \mathbf{D} \end{bmatrix}^{(j-1)} \tag{1}$$

Increasing laminate thickness shifts the mid-plane position and consequently alters ply coordinates. For a single-ply thickness of t, adding one sub-ply comprising four plies induces a mid-plane shift of $2t$, as illustrated in Figure 2. Thus, the difference in laminate ABD matrices can be formulated as:

$$\begin{aligned}
\Delta\mathbf{A}^{(j)} &= \mathbf{A}^{(j)} - \mathbf{A}^{(j-1)} = \sum_{k=n+1}^{n+4} \overline{\mathbf{Q}}_k \left(Z_k^{(j)} - Z_{k-1}^{(j)} \right) \\
\Delta\mathbf{B}^{(j)} &= \mathbf{B}^{(j)} - \mathbf{B}^{(j-1)} = -2t\mathbf{A}^{(j-1)} + \sum_{k=n+1}^{n+4} \overline{\mathbf{Q}}_k \frac{\left(Z_k^{(j)}\right)^2 - \left(Z_{k-1}^{(j)}\right)^2}{2} \\
\Delta\mathbf{D}^{(j)} &= \mathbf{D}^{(j)} - \mathbf{D}^{(j-1)} = -4t\mathbf{B}^{(j-1)} + 4t^2\mathbf{A}^{(j-1)} + \sum_{k=n+1}^{n+4} \overline{\mathbf{Q}}_k \frac{\left(Z_k^{(j)}\right)^3 - \left(Z_{k-1}^{(j)}\right)^3}{3}
\end{aligned} \tag{2}$$

Where k is the ply number, Z^k and $Z^{k\text{-}1}$ are the coordinates of the upper and lower surfaces of the new ply, and $\overline{\mathbf{Q}}$ is the unidirectional plate off-axis stiffness matrix.

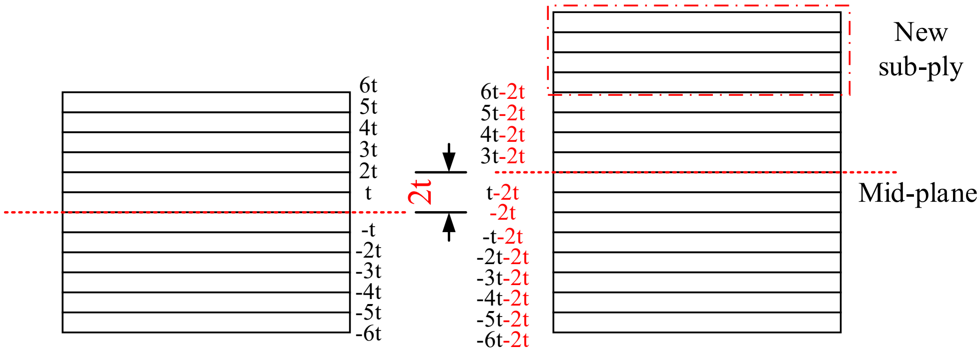

Figure 2: Schematic diagram of the mid-plane and plies coordinates changes in the thickness variation of DD laminates.

The improved weight expression comprises only two multiplicative terms. The first term raises the design variable of the current sub-ply to the power of p to ensure convergence to 0 or 1. The second term equals the product of design variables within the local search area of the underlying sub-ply. This formulation ensures gradual thickness tapering and prevents the occurrence of intermediate empty sub-plies. In the improved PPI model, the weight w_{ij} of the sub-ply jth in the element ith can be expressed as:

$$w_{ij} = x_{ij}^{p} \prod_{k\in\Omega} x_{kj-1} \tag{3}$$

The model ensures gradual thickness tapering. Specifically, the existence of sub-ply jth presupposes the existence of sub-ply j-1th to prevent empty sub-plies. Similarly, sub-ply j-1th depends on sub-ply j-2th. This recursive dependency ensures that if sub-ply jth exists, all underlying sub-plies remain present without voids.

2.2 Continuous angle

Continuous angle optimisation is achieved by establishing the relationship between ply angles and laminate stiffness matrices. The laminate **ABD** matrices are derived by integrating the off-axis stiffness matrix $\overline{\mathbf{Q}}$ along the thickness direction. The off-axis stiffness matrix is obtained by transforming the on-axis stiffness matrix using the rotation matrix.

$$\overline{\mathbf{Q}_k} = \mathbf{T}_k \mathbf{Q}_k \mathbf{T}_k^{\mathrm{T}} \tag{4}$$

Here, $\mathbf{T}$ denotes the rotation matrix about the Z-axis, and its relationship with the angle θ_k is defined as:

$$\mathbf{T}(\theta_k) = \begin{bmatrix} \cos^2\theta_k & \sin^2\theta_k & -2\cos\theta_k\sin\theta_k \\ \sin^2\theta_k & \cos^2\theta_k & 2\cos\theta_k\sin\theta_k \\ \cos\theta_k\sin\theta_k & -\cos\theta_k\sin\theta_k & \cos^2\theta_k - \sin^2\theta_k \end{bmatrix} \tag{5}$$

2.3 Discrete angle penalty strategy

To obtain discrete DD ply angles in the final results, a penalty is imposed on intermediate angles by introducing an angle weight coefficient to the off-axis stiffness matrix. The weight equals unity for selected discrete angles and is less than one for intermediate values.

$$\overline{\mathbf{Q}_k^w} = w_k^{(\theta)} \overline{\mathbf{Q}_k} \tag{6}$$

This work proposes two discrete ply angle penalty strategies, specifically the linear strategy and the trigonometric function penalty strategy.

$$w_k^{(\theta)} = \begin{cases} -A\left(x_k^{(\theta)} - \dfrac{i}{N_{\mathrm{d}}}\right) + 1 & \left(\dfrac{i}{N_{\mathrm{d}}} \le x_k^{(\theta)} < \dfrac{i}{N_{\mathrm{d}}} + \dfrac{1}{2N_{\mathrm{d}}}\right) \\ A\left(x_k^{(\theta)} - \dfrac{i+1}{N_{\mathrm{d}}}\right) + 1 & \left(\dfrac{i}{N_{\mathrm{d}}} + \dfrac{1}{2N_{\mathrm{d}}} \le x_k^{(\theta)} < \dfrac{i+1}{N_{\mathrm{d}}}\right) \end{cases} \tag{7}$$

i : Integer within the range of 0 to N_{d} - 1.

$$w_k^{(\theta)} = A\cos\left(2N_{\mathrm{d}}\pi x_k^{(\theta)}\right) + (1 - A) \tag{8}$$

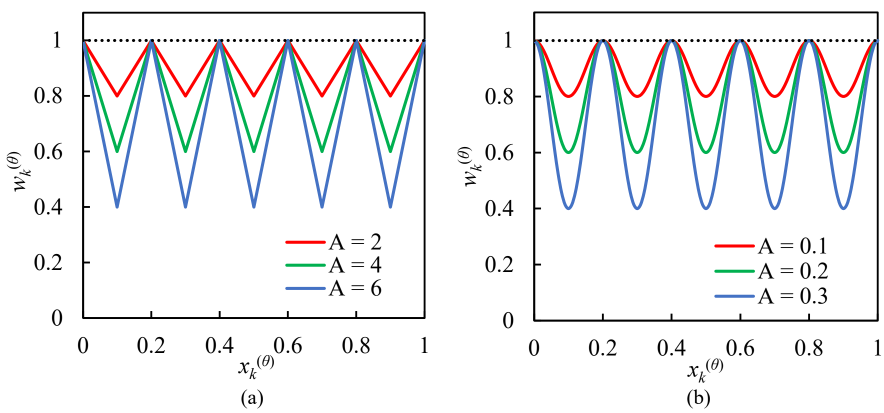

Figure 3: Discrete DD ply angles penalty strategy: (a)Linear penalty strategy, (b) Trigonometric penalty strategy

Here, $x_k^{(\theta)}$ denotes the angle design variable ranging from 0 to 1. N_d represents the number of discrete DD ply angles, which are selected within the range of 0° to 90°. For instance, when N_d=3, the discrete angles are set to 0°, 30°, 60°, and 90°. The index i is an integer varying from 0 to N_d-1, and A controls the penalty intensity. The figure below illustrates the curves of angle weight versus angle design variable for the linear penalty strategy with A=2, 4, 6, and the trigonometric penalty strategy with A=0.1, 0.2, 0.3, when N_d=5.

3 Description of the optimisation problem

Under the volume fraction constraint, the compliance minimization problem is formulated as:

$$\begin{aligned}
&\text{find}: \left\{x_{ij}, x_{\Phi}^{(\theta)}, x_{\Psi}^{(\theta)}\right\} \quad \left(i=1,\ \dots\ ,n_{\mathrm{e}}; j=1,\ \dots\ ,n_{\mathrm{sp}}\right)\\
&\text{minimize}: \ C = \mathbf{F}^{\mathrm{T}}\mathbf{u}\\
&\text{subject to}: \ \mathbf{F} = \mathbf{K}\mathbf{u}\\
&\qquad \frac{\sum x_{ij}V_{ij}}{\sum V_{ij}} \le vof
\end{aligned} \tag{9}$$

Herein, x_{ij} represents the design variable of the thickness, where x_{ij}=1 indicates that the jth sub-ply exists in the ith element, and x_{ij}=0 indicates that it does not. The number of elements is denoted as n_e, and the number of alternative DD sub-plies is represented by n_{sp}. C stands for the overall compliance. **K** is the element stiffness matrix. **F** is the external force vector. **u** is the displacement vector. V represents the volume, and vof represents the volume fraction.

While element-wise angle optimisation is theoretically feasible, it remains impractical under current manufacturing constraints due to strict requirements for fibre continuity and angle variations. Therefore, this work employs a global set of designable DD ply angles [±Φ/±Ψ] for the entire structure, where Φ and Ψ serve as the design variables.

3.2 Sensitivity analysis

The overall compliance sensitivity can typically be represented as:

$$\frac{\partial C}{\partial x_{ij}} = 2\mathbf{u}^{\mathrm{T}}\frac{\partial \mathbf{F}}{\partial x_{ij}} - \mathbf{u}^{\mathrm{T}}\frac{\partial \mathbf{K}}{\partial x_{ij}}\mathbf{u} \tag{10}$$

For fixed loads, then we have $\partial \boldsymbol{F}/\partial x_{ik} \equiv 0$. Thus, the sensitivity can be simplified as:

$$\frac{\partial C}{\partial x_{ij}} = -\mathbf{u}^{\mathrm{T}}\frac{\partial \mathbf{K}}{\partial x_{ij}}\mathbf{u} = -\mathbf{u}_i^{\mathrm{T}}\frac{\partial \mathbf{K}_i}{\partial x_{ij}}\mathbf{u}_i - \sum_{s\in\Omega_i}\mathbf{u}_s^{\mathrm{T}}\frac{\partial \mathbf{K}_s}{\partial x_{ij}}\mathbf{u}_s \tag{11}$$

Where Ω_i represents the element in the ith element's local search area, $\mathbf{K}_i$ and $\mathbf{K}_s$ are the stiffness matrix of the ith element and the elements in the local search area, can be defined as:

$$\mathbf{K}_i = \iint \begin{bmatrix} \mathbf{B}_\mathrm{p} \\ \mathbf{B}_\mathrm{b} \end{bmatrix}_i^\mathrm{T} \begin{bmatrix} \mathbf{A} & \mathbf{B} \\ \mathbf{B} & \mathbf{D} \end{bmatrix}_i \begin{bmatrix} \mathbf{B}_\mathrm{p} \\ \mathbf{B}_\mathrm{b} \end{bmatrix}_i dxdy \tag{12}$$

Where $\left[\mathbf{B}_\mathrm{p}\right]$ and $\left[\mathbf{B}_\mathrm{b}\right]$ are relations between strain and displacement vectors.

$$\{\boldsymbol{\kappa}\} = \left[\mathbf{B}_\mathrm{b}\right]\{\mathbf{u}_\mathrm{b}\};\ \{\boldsymbol{\varepsilon}^0\} = \left[\mathbf{B}_\mathrm{p}\right]\{\mathbf{u}_\mathrm{p}\} \tag{13}$$

$\boldsymbol{\varepsilon}^0$ is the middle plane strain vector, $\boldsymbol{\kappa}$ is the middle plane curvature vector. According to the derivation of Eq.(12), the sensitivity of the thickness variable $\partial \mathbf{K}_i / \partial x_{ij}$ can be expressed as:

$$\frac{\partial \mathbf{K}_i}{\partial x_{ij}} = \iint \begin{bmatrix} \mathbf{B}_p \\ \mathbf{B}_b \end{bmatrix}_i^\mathrm{T} \left(\sum_{n=1}^{n_\mathrm{sp}} \frac{\partial w_{in}}{\partial x_{ij}} \begin{bmatrix} \Delta\mathbf{A} & \Delta\mathbf{B} \\ \Delta\mathbf{B} & \Delta\mathbf{D} \end{bmatrix}_i^{(n)} \right) \begin{bmatrix} \mathbf{B}_p \\ \mathbf{B}_b \end{bmatrix}_i dxdy \tag{14}$$

Mathematically, the following relation can easily be derived:

$$\frac{\partial \mathbf{K}_i}{\partial x_{ij}} = \sum_{n=1}^{n_\mathrm{sp}} \frac{\partial w_{in}}{\partial x_{ij}} \iint \begin{bmatrix} \mathbf{B}_\mathrm{p} \\ \mathbf{B}_\mathrm{b} \end{bmatrix}_i^\mathrm{T} \begin{bmatrix} \Delta\mathbf{A} & \Delta\mathbf{B} \\ \Delta\mathbf{B} & \Delta\mathbf{D} \end{bmatrix}_i^{(n)} \begin{bmatrix} \mathbf{B}_\mathrm{p} \\ \mathbf{B}_\mathrm{b} \end{bmatrix}_i dxdy = \sum_{n=1}^{n_\mathrm{sp}} \frac{\partial w_{in}}{\partial x_{ij}} \Delta\mathbf{K}_i^{(n)} \tag{15}$$

To calculate the partial derivative of weight w, the interpolation model given is used to produce.

$$\frac{\partial w_{in}}{\partial x_{ij}} = \begin{cases} 0 & \text{if } j < n-1 \\ x_{in}^p \prod\limits_{\substack{k\in\Omega \\ k\neq 1}} x_{kn-1} & \text{if } j = n-1 \\ p x_{ij}^{p-1} \prod\limits_{k\in\Omega} x_{kn-1} & \text{if } j = n \\ 0 & \text{if } j > n \end{cases} \tag{16}$$

The sensitivity of the continuous angle variable can be expressed as:

$$\begin{aligned} \frac{\partial \mathbf{K}_i}{\partial x_\Phi^{(\theta)}} &= \iint \begin{bmatrix} \mathbf{B}_p \\ \mathbf{B}_b \end{bmatrix}_i^\mathrm{T} \left(\frac{\partial}{\partial \theta_\Phi} \left(\sum_{j=1}^{m_L} w_{ij} \Delta \begin{bmatrix} \mathbf{A} & \mathbf{B} \\ \mathbf{B} & \mathbf{D} \end{bmatrix}_i^{(j)} + \begin{bmatrix} \mathbf{A} & \mathbf{B} \\ \mathbf{B} & \mathbf{D} \end{bmatrix}_i^{(0)} \right) \frac{\partial \theta_\Phi}{\partial x_\Phi^{(\theta)}} \right) \begin{bmatrix} \mathbf{B}_p \\ \mathbf{B}_b \end{bmatrix}_i dxdy \\ \frac{\partial \mathbf{K}_i}{\partial x_\Psi^{(\theta)}} &= \iint \begin{bmatrix} \mathbf{B}_p \\ \mathbf{B}_b \end{bmatrix}_i^\mathrm{T} \left(\frac{\partial}{\partial \theta_\Psi} \left(\sum_{j=1}^{m_L} w_{ij} \Delta \begin{bmatrix} \mathbf{A} & \mathbf{B} \\ \mathbf{B} & \mathbf{D} \end{bmatrix}_i^{(j)} + \begin{bmatrix} \mathbf{A} & \mathbf{B} \\ \mathbf{B} & \mathbf{D} \end{bmatrix}_i^{(0)} \right) \frac{\partial \theta_\Psi}{\partial x_\Psi^{(\theta)}} \right) \begin{bmatrix} \mathbf{B}_p \\ \mathbf{B}_b \end{bmatrix}_i dxdy \end{aligned} \tag{17}$$

$$\frac{\partial \mathbf{T}}{\partial \theta} = \begin{bmatrix} -\sin 2\theta & \sin 2\theta & -2\cos 2\theta \\ \sin 2\theta & -\sin 2\theta & 2\cos 2\theta \\ \cos 2\theta & -\cos 2\theta & -2\sin 2\theta \end{bmatrix} \tag{18}$$

The sensitivity of the discrete angle is

$$\frac{\partial \overline{\mathbf{Q}_k^w}}{\partial x_k^{(\theta)}} = \frac{\partial w_k^{(\theta)}}{\partial x_k^{(\theta)}} \overline{\mathbf{Q}}_k + w_k^{(\theta)} \frac{\partial \overline{\mathbf{Q}}_k}{\partial \theta} \frac{\partial \theta}{\partial x_k^{(\theta)}} \tag{19}$$

To the linear strategy and the trigonometric function penalty strategy:

$$\frac{\partial w_k^{(\theta)}}{\partial x_k^{(\theta)}} = \begin{cases} -A & \left(\frac{i}{N_\mathrm{d}} \le x_k^{(\theta)} < \frac{i}{N_\mathrm{d}} + \frac{1}{2N_\mathrm{d}}\right) \\ A & \left(\frac{i}{N_\mathrm{d}} + \frac{1}{2N_\mathrm{d}} \le x_k^{(\theta)} < \frac{i+1}{N_\mathrm{d}}\right) \end{cases} \tag{20}$$

$$\frac{\partial w_k^{(\theta)}}{\partial x_k^{(\theta)}} = -2AN_\mathrm{d}\pi \sin(2N_\mathrm{d}\pi x_k^{(\theta)}) \tag{21}$$

4 Numerical example

The effectiveness of the proposed method for simultaneous angle and thickness optimisation of DD laminates is validated through numerical examples: an aircraft fuselage skin. The implementation is coded in FORTRAN, finite element analysis is performed using the SHELL99 element in ANSYS, and the optimisation algorithm employs GCMMA. The optimisation procedure is deemed convergent when the relative change in the objective function value remains below 0.1% for five successive iterations.

4.1 The aircraft fuselage lower skin

The aircraft fuselage lower skin, as illustrated in : , features a trapezoidal panel with complex curvature. The boundary conditions are defined as riveted constraints along all four edges, subjected to aerodynamic pressure loads. The 0° direction aligns with the fuselage axial direction.

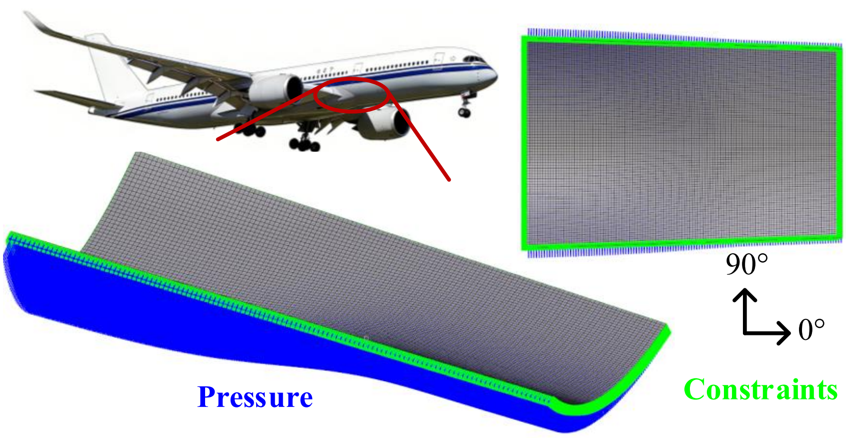

Figure 4: Finite element model and boundary conditions of the aircraft fuselage lower skin

The taper ratio is set to 1:100, and the volume fraction constraint is fixed at 0.6. Optimisation results for the aircraft fuselage lower skin are computed for both continuous ply angles and discrete ply angles with a 7.5° increment. Both the linear penalty strategy and the trigonometric function penalty strategy are effective for enforcing discrete ply angles, with comparable performance. The linear penalty strategy is adopted in this numerical example. The optimisation results are illustrated in Figure 5, where different colours denote different numbers of sub-plies.

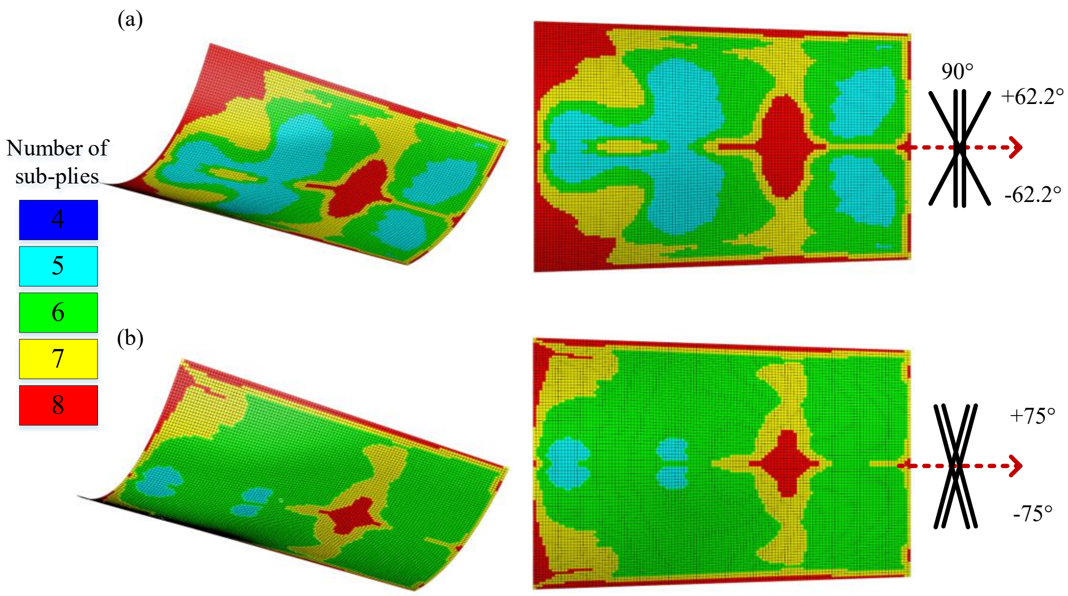

Figure 5: Optimisation results of the fuselage lower skin: (a) Continuous ply angle optimisation; (b) Discrete ply angle optimisation.

The layout patterns of the two optimisation results exhibit notable differences. The continuous angle optimisation yields a larger distribution area of the thickest sub-plies (8 sub-plies), whereas the discrete angle optimisation features a more extensive distribution of intermediate thickness sub-plies (6 sub-plies).

The compliance and ply angle convergence curves are presented in Figure 6 and Figure 7, respectively. The compliance converges steadily, with continuous and discrete ply angles reaching convergence at iterations 79 and 87, respectively. In terms of compliance values, the difference between the two optimisation results is marginal, with a relative discrepancy of less than 1%. The optimized continuous ply angles converge to [62.2°, -90°,-62.2°, 90°], while the discrete ply angles converge to [75°, -75°, -75°, 75°]. Minor fluctuations are observed during the convergence process, which can be attributed to the high nonlinearity inherent in angle optimisation. Ultimately, all angle variables stabilize at their final values.

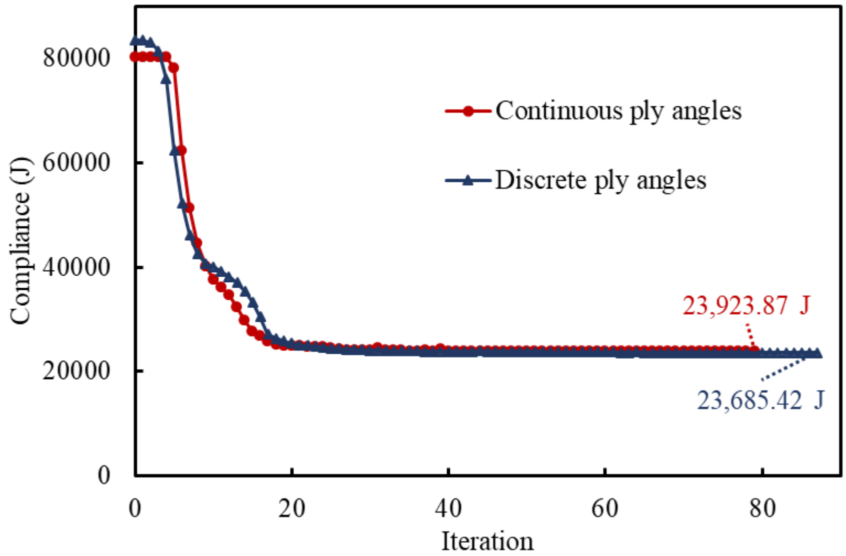

Figure 6: Compliance convergence curve of the fuselage lower skin

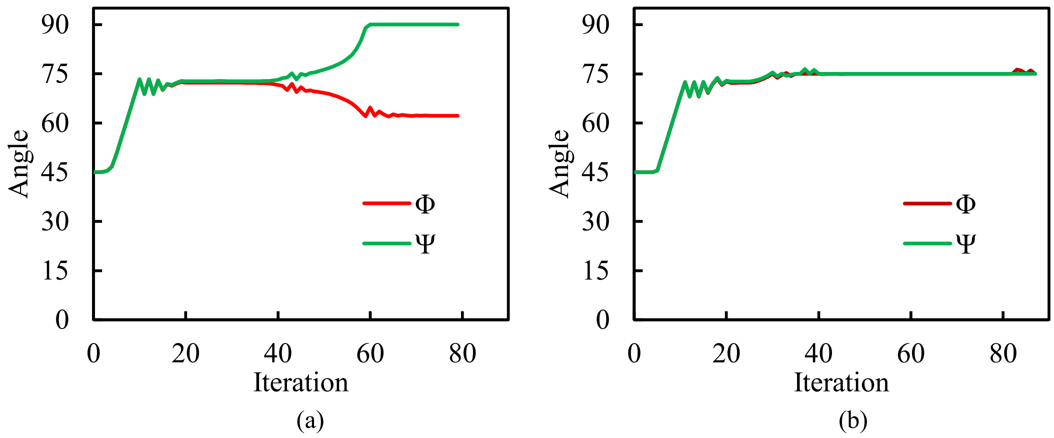

Figure 7: Angle convergence curve: (a) Continuous ply angle optimisation; (b) Discrete ply angle optimisation.

5 Conclusion

This work proposes a simultaneous optimisation method for ply angles and thickness of Double-Double (DD) laminates. Specifically, the Progressive Ply Interpolation (PPI) model is enhanced by embedding angle optimisation into the interpolation framework. This enables concurrent design of DD laminate angles and thickness. Furthermore, two discrete ply angle penalty strategies are introduced to ensure discrete angle values. Optimisation results demonstrate the effectiveness of these strategies in achieving discrete ply angles.

Acknowledgements

This work is supported by the Fundamental and Interdisciplinary Disciplines Breakthrough Plan of the Ministry of Education of China (JYB2025XDXM207) and the National Natural Science Foundation of China (U2441208).

References

[1] P. Fang, T. Gao, S. Gao, Y. Huang, W. Zhang, The progressive ply interpolation model for the optimisation design of double-double laminates with gradual thickness tapering, Computers & Structures 315 (2025) 107790.

[2] S.W. Tsai, Double–Double: New Family of Composite Laminates, AIAA Journal 59 (2021) 4293–4305.

[3] S.W. Tsai, W.E. Guin, A. Riccio, Weight and cost reduction with double-double laminates, (n.d.) 3.

[4] E. Kappel, Double–Double laminates for aerospace applications — Finding best laminates for given load sets, Composites Part C: Open Access 8 (2022) 100244.

[5] S. Shrivastava, N. Sharma, S.W. Tsai, P.M. Mohite, D and DD-drop layup optimisation of aircraft wing panels under multi-load case design environment, Composite Structures 248 (2020) 112518.

[6] D. Zerbst, L. Tönjes, S. Dähne, E. Werthen, E. Kappel, C. Hühne, Equivalent plate formulation of Double–Double laminates for the gradient-based design optimisation of composite structures, Composite Structures 354 (2025) 118786.

[7] Y. Wang, D. Wang, Y. Zhong, D.W. Rosen, S. Li, S.W. Tsai, Topology optimisation of Double-Double (DD) composite laminates considering stress control, Computer Methods in Applied Mechanics and Engineering 414 (2023) 116191. https://doi.org/10.1016/j.cma.2023.116191.